TEXAS
The University of Texas at Austin

Texas Trauma Service Area (TSA) COVID-19 transmission estimates and healthcare projections

Michael Lachmann, Spencer J. Fox, Mauricio Tec, Remy Pasco, MaureenJohnson, Jenny Lu, Zhanwei Du, Spencer Woody, Jennifer Starling, Maytal Dahan, Kelly Gaither, Kelly Pierce, James Scott, Gordon Wells, Lauren Ancel Meyers

The University of Texas at Austin
COVID-19 Modeling Consortium

utpandemics@austin.utexas.edu

Texas Trauma Service Area (TSA) COVID-19 transmission estimates and healthcare projections

Presented to the Texas Department of State Health Services on August 1, 2020

[The University of Texas COVID-19 Modeling Consortium]

Contributors: Michael Lachmann*, Spencer J. Fox*, Mauricio Tec*, Remy Pasco, Maureen Johnson, Jenny Lu, Zhanwei Du, Spencer Woody, Jennifer Starling, Maytal Dahan, Kelly Gaither, Kelly Pierce, James Scott, Gordon Wells, Lauren Ancel Meyers

* Contributed equally

Contact: utpandemics@austin.utexas.edu

Overview

To support public health decision-making and healthcare planning, we developed a model that can provide real-time estimates of the prevalence and transmission rate of COVID-19 and project healthcare needs into the future for each of the 22 Trauma Service Areas (TSA) in Texas.

The model incorporates key epidemiological characteristics of the disease, demographic information for each TSA, and local mobility data from anonymized cell phone traces. It uses daily COVID-19 hospitalization data to estimate the changing transmission rate and prevalence of disease. The framework can be readily applied to provide pandemic situational awareness and short-term healthcare projections in other cities around the US.

In this report, we use COVID-19 hospitalization data for each TSA from April 11 to July 22, 2020 to estimate the state of the pandemic in late July and project hospitalizations through early August of 2020. The data were provided by Texas DSHS through daily and weekly reports as summarized in the Texas 2036 dashboard. We note two limitations with these data that could bias our projections. First, data are not available before April 11th. Second, the ratio between COVID-19 hospital admissions and hospitalizations is variable across TSA regions. Thus, there may be regional differences in reporting confirmed COVID-19 hospital admissions which are not explicitly considered in the projections below. In addition, the projections are based on multiple assumptions about the age-specific severity of COVID-19 and the role of asymptomatic infections in the transmission of the virus. These graphs below do not present the full range of uncertainty, but are intended to provide basic insight into the changing risks of COVID-19 transmission and healthcare surges in each TSA.

Our estimates suggest that every TSA has experienced a recent surge in cases, hospitalizations, and mortality, with transmission starting to rise in early May. Many regions are now seeing declining numbers. In four TSA's, covering the largest metropolitan areas, the data indicate over a 90% chance that the current wave is subsiding (TSA's E, I, P, and Q). Our projections suggest that the only region with over a 90% chance that the current pandemic wave is still growing is Waco. In the remaining 17 TSA's, the future is more uncertain. COVID-19 is straining healthcare systems across the state. Although most TSA's are at low risk for reaching total hospital bed capacity, several could exceed ICU capacity. Only the Dallas, Paris, El Paso, Midland/Odessa, Austin, San Antonio, and Houston regions have at least 90% certainty of remaining within their ICU bed capacity over the next 3 weeks.

We are posting these results prior to peer review to provide intuition for both policy makers and the public regarding both the immediate threat of COVID-19 and the extent to which continued social distancing, transmission-reducing precautions such as keeping physical distance, wearing cloth face coverings and staying isolated when symptomatic, can mitigate that threat.

As new hospitalization data become available, we will provide updated estimates and projections on the UT COVID-19 Modeling Consortium's website.

COVID-19 Model for Texas Trauma Service Areas

The appendix below describes the model in detail. In short, we use mathematical equations to track the changing numbers of individuals who are susceptible (not yet infected), infected, hospitalized, recovered, and deceased. The model incorporates key features of the virus and uses iterated filtering [1] to estimate daily transmission rates in each TSA from a combination of local COVID-19 hospital admissions data as well as SafeGraph mobility trends (cell phone-based estimates of hours spent at home and daily trips to public points-of-interest such as grocery stores, restaurants, bars and parks [2]). We use the estimated transmission rates to project COVID-19 cases, hospitalizations, and ICU visits several weeks ahead. The model makes the following assumptions:

- Pandemic seeding: Projections begin on April 11. The numbers of infected people in each age group on that date are estimates from statewide hospitalization data.
- Following infection, cases go through multiple stages of infection:

  Stage 1: Pre-symptomatic and non-contagious for an average of 2.9 days

  Stage 2: Pre-symptomatic and contagious for an average of 2.3 days (44% of transmission events occur during this period)

  Stage 3: Symptomatic and contagious or asymptomatic and contagious for an average of 4 days. The model assumes that 57% of all infections become symptomatic (43%

remain asymptomatic) and that asymptomatic cases are 67% as infectious as symptomatic cases.

- Cases may be hospitalized and released/die.
    - The overall infection hospitalization rate (IHR) is 4.2%.
    - Since the length of COVID-19 hospital stays and the COVID-19 mortality rates have been changing, we allow these numbers to vary based on the data.

COVID-19 transmission through July 22, 2020

We track COVID-19 spread through a quantity called the effective reproduction number, $R(t)$. This indicates the contagiousness of the virus at a given point time and roughly corresponds to the average number of people a typical case will infect. Measures to slow or prevent transmission, such as social distancing and mask wearing, can reduce the reproduction number. Immunity acquired either through past infection or vaccination can also reduce the reproduction number. If $R(t)$ is greater than one, then an epidemic will continue to grow; if $R(t)$ is less than one, it will begin to subside. By tracking $R(t)$, we can detect whether policies and individual-level behaviors are having the desired impact and project cases, hospitalizations and deaths into the future.

In many TSA's, the effective reproduction number of COVID-19 increased following the relaxation of March-April stay-home orders. The estimates peak in mid-June and then decline into early July. At the mid-June peaks, we estimate effective reproduction numbers ranging from close to one in Paris to over two in El Paso, San Antonio, Wichita Falls, Abilene, Corpus Christi, Victoria, and Laredo.

Table 1 provides the probability that the current epidemic wave is declining, for each TSA. The risks are heterogeneous across the state. Four regions are highly likely to have declining epidemics (with probability of decline over 90%): Dallas/Fort Worth, El Paso, San Antonio, and Houston. Only Waco has at least 90% certainty that the epidemic is still growing. The trends in the remaining regions are more uncertain. Aggregating across all 22 TSA's, the model projects that the recent surge in COVID-19 transmission across Texas is declining, with 95% probability.

Table 1 also provides estimates for COVID-19 prevalence in each TSA and statewide. As of July 22nd, the current prevalence of COVID-19 statewide is estimated at 7.8 (95% CrI: 7.1-8.6) per 1,000 and the cumulative proportion of the state population that has been infected is 10.6% (95% CrI: 10.2%-10.9%). The regional risks vary. The estimated current prevalence exceeds 1% of the population in seven TSA's and cumulative cases exceeding 10% of the population in ten TSA's. Waco has the highest estimated cumulative incidence of 14.7% (95%CrI: 13.0%-16.8%) of people infected, followed by the Lower Rio Grande valley with 14.0% (95% CrI: 12.6%-15.5%), and Dallas/Fort Worth with 13.7% (95% CrI: 13.0%-14.5%).

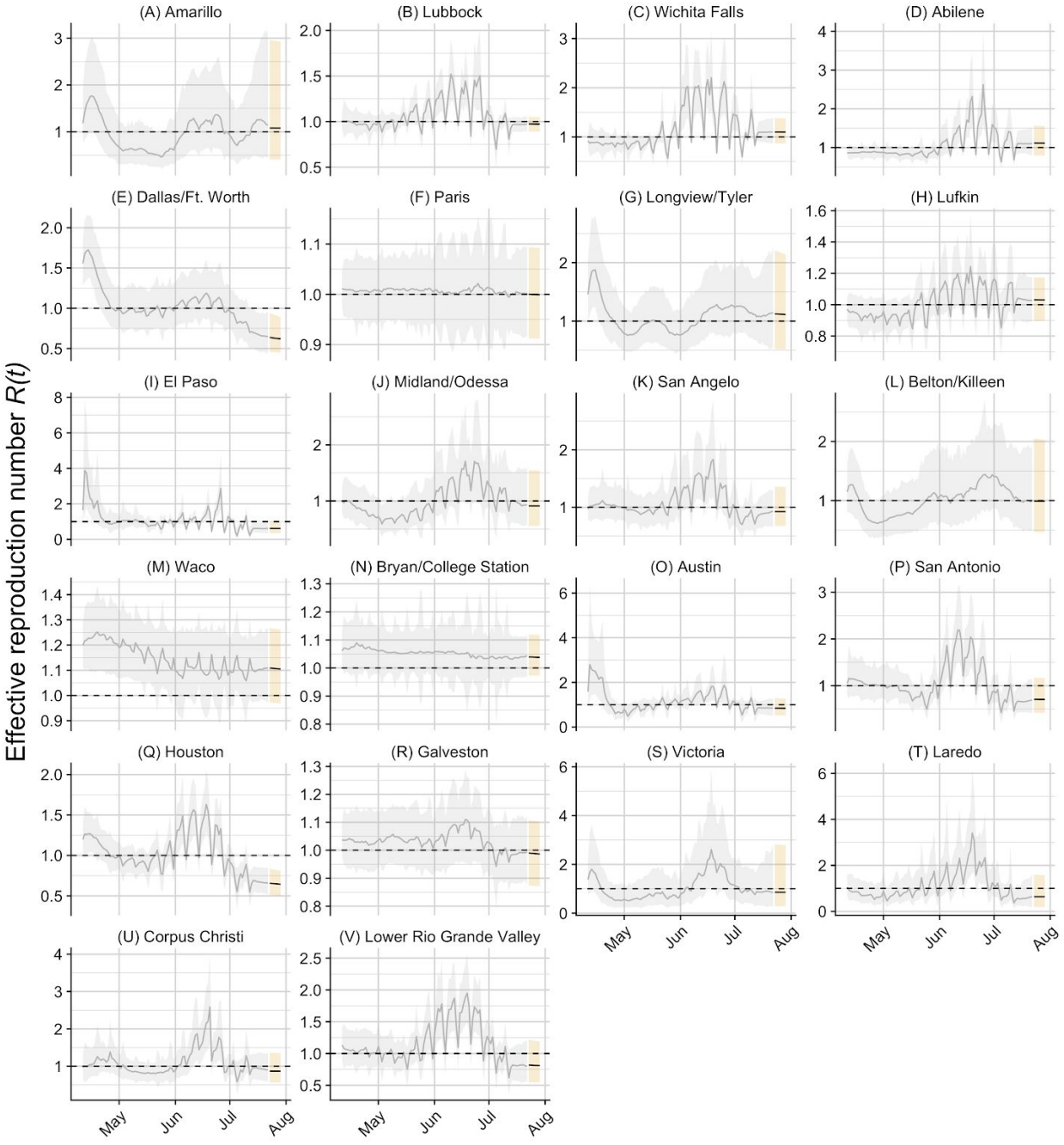

Figure 1: The estimated effective reproduction number, *R*(*t*), of the COVID-19 pandemic in each TSA, April 11-July 29, 2020. *R*(*t*) is an epidemiological quantity used to describe the contagiousness of a disease. An epidemic is expected to continue if *R*(*t*) is greater than one and to end if *R*(*t*) is less than one. This *epidemic threshold* of *R*(*t*) = 1 is indicated by a horizontal dashed line. *R*(*t*) can be interpreted as the average number of people that an infected case will infect. The value of *R*(*t*) depends on the basic infectiousness of the disease, the number of people that are susceptible to infection, and the impact of social distancing, mask wearing and other measures to slow transmission. The solid lines give the mean daily estimates and the shaded ribbons indicate the 95% credible intervals.

Table 1: COVID-19 estimates for Texas TSA's as of July 22, 2020. Numbers in parentheses are 95% credible intervals.

TSA	Region	R_t	Probability epidemic declining	Current prevalence (Infections per 1,000)	Cumulative Incidence
A	Amarillo	1.23 (0.41-2.95)	43.4%	3.4 (1.3-7)	6.2% (5.3%-7.3%)
B	Lubbock	0.97 (0.89-1.05)	71.2%	8 (6.4-9.9)	7.7% (6.8%-8.7%)
C	Wichita Falls	1.1 (0.87-1.38)	20.4%	11.8 (7.7-17.2)	6.9% (5.6%-8.5%)
D	Abilene	1.14 (0.8-1.57)	25.4%	16.6 (8.9-29.9)	11.3% (8.8%-15.3%)
E	Dallas/Ft. Worth	0.65 (0.46-0.94)	99.2%	7.6 (5.9-9.7)	13.7% (13.0%-14.5%)
F	Paris	1 (0.91-1.09)	49.6%	7.6 (5.7-10)	10.4% (9.5%-11.6%)
G	Longview/Tyler	1.19 (0.52-2.2)	39.0%	13.1 (8.6-19.2)	11.5% (10.4%-12.9%)
H	Lufkin	1.03 (0.9-1.17)	33.0%	5.9 (4.1-8.3)	6.8% (5.9%-7.8%)
I	El Paso	0.63 (0.35-1.01)	96.8%	5.1 (3.4-7.4)	9.7% (8.8%-10.5%)
J	Midland/Odessa	0.95 (0.55-1.55)	62.6%	3.5 (1.8-5.8)	3.4% (2.8%-4.0%)
K	San Angelo	0.95 (0.67-1.36)	66.0%	9.6 (4.6-18.3)	10.0% (7.2%-13.6%)
L	Belton/Killeen	1.05 (0.46-2.05)	50.8%	8.8 (4.8-16.1)	7.4% (6.2%-9.1%)
M	Waco	1.11 (0.97-1.27)	5.6%	18.2 (13.7-24.2)	14.7% (13.0%-16.8%)
N	Bryan/College Station	1.04 (0.97-1.12)	14.8%	7.9 (6.3-9.7)	8.8% (7.8%-9.8%)
O	Austin	0.86 (0.52-1.29)	76.4%	5.1 (3.3-7.4)	4.8% (4.3%-5.5%)
P	San Antonio	0.73 (0.42-1.17)	91.0%	4.1 (2.8-5.9)	6.1% (5.5%-6.7%)
Q	Houston	0.66 (0.51-0.83)	100.0%	7.3 (5.7-9)	12.3% (11.4%-13.3%)
R	Galveston	0.99 (0.87-1.11)	55.4%	5.3 (4.1-6.7)	6.4% (5.8%-7.2%)
S	Victoria	1.02 (0.28-2.81)	59.8%	15.2 (7.3-28.2)	13.2% (11.1%-16.5%)
T	Laredo	0.71 (0.19-1.58)	81.2%	6.4 (3.2-12.4)	6.3% (5.2%-7.8%)
U	Corpus Christi	0.9 (0.56-1.36)	73.0%	14.1 (9.4-20.1)	12.0% (10.6%-13.6%)
V	Lower Rio Grande Valley	0.83 (0.55-1.21)	85.2%	17.4 (12.4-23.7)	14.0% (12.6%-15.5%)
	Statewide	NA	95.0%	7.8 (7.1-8.6)	10.6% (10.2%-10.9%)

COVID-19 healthcare projections

Based on data through the third week of July, we project the numbers of COVID-19 hospitalizations and ICU patients through August 12th (Figures 2 and 3). These trends are driven by the underlying transmission rates estimated in Figure 1 and Table 1. Our *spaghetti line* projections in each figure indicate uncertainty in our projects. Some trend upwards while others trend downwards. Each line represents an equally likely future path. The bold line in each graph indicates the median across the different trends.

For each TSA, we calculated both the hospital and ICU-specific bed capacities by summing DSHS estimates for bed usage and available beds on July 22, 2020. Note that these estimates do not account for potential surge capacity. Figure 2 suggests that many regions appear to have sufficient hospital bed capacity for the projected demand through August 12th. The risk that COVID-19 hospitalizations will exceed capacity within the next three weeks is highest in Corpus Christi (40%), followed by Waco and Longview/Tyler (30%) (Table 2).

Our projections in Figure 3 suggest that COVID-19 cases are likely to exceed ICU capacities before they exceed total hospital capacities. Only seven TSA's have less than a 10% chance of exceeding ICU capacity within the next three weeks: Dallas, Paris, El Paso, Midland/Odessa, Austin, San Antonio, and Houston (Table 2).

Table 2: COVID-19 healthcare projections for Texas Trauma Service Areas as of July 22, 2020.

TSA	Region	Probability exceed hospital capacity within 3 weeks	Probability exceed ICU capacity within 3 weeks
A	Amarillo	15%	46%
B	Lubbock	0%	28%
C	Wichita Falls	5%	46%
D	Abilene	0%	41%
E	Dallas/Ft. Worth	0%	0%
F	Paris	0%	0%
G	Longview/Tyler	30%	46%
H	Lufkin	4%	18%
I	El Paso	0%	1%
J	Midland/Odessa	0%	3%
K	San Angelo	2%	28%
L	Belton/Killeen	16%	58%
M	Waco	30%	58%
N	Bryan/College Station	0%	18%
O	Austin	2%	7%
P	San Antonio	0%	1%
Q	Houston	0%	0%
R	Galveston	26%	52%
S	Victoria	37%	46%
T	Laredo	6%	11%
U	Corpus Christi	40%	67%
V	Lower Rio Grande Valley	7%	16%

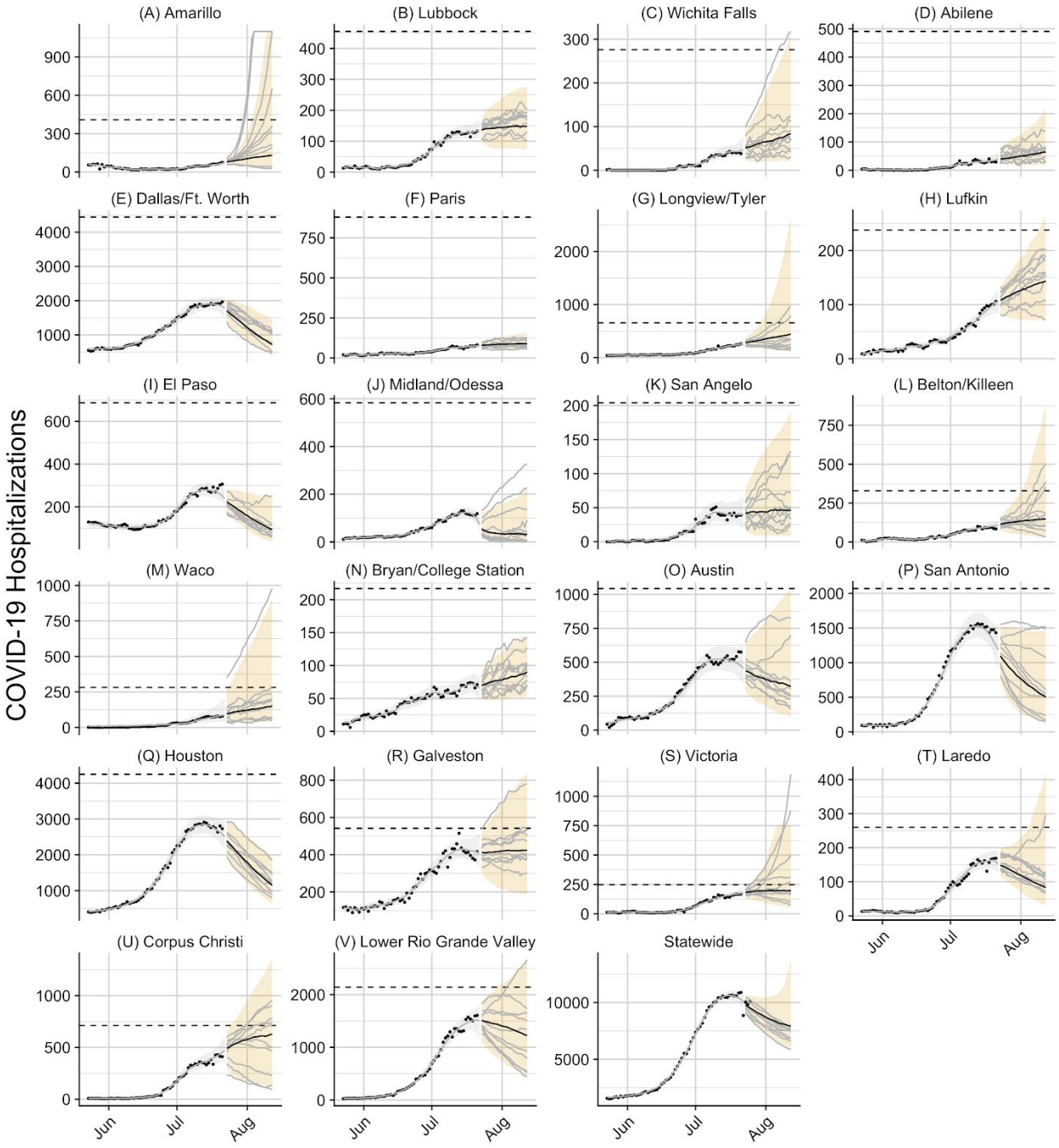

Figure 2: Projected COVID-19 hospitalizations through August 12, 2020 by TSA. Black points represent the reported daily COVID-19 hospital census provided by DSHS. Grey "spaghetti" lines represent equally likely projections and the black lines indicate the median trend based on the range of transmission rates estimated for July 22-August 12, 2020 (Figure 1). Differences between lines are caused by uncertainty in the model inputs as well as variation in individual behavior and disease progression. Horizontal dashed lines indicate the estimated TSA-specific hospitalization bed capacity (obtained by summing used and available hospital beds).

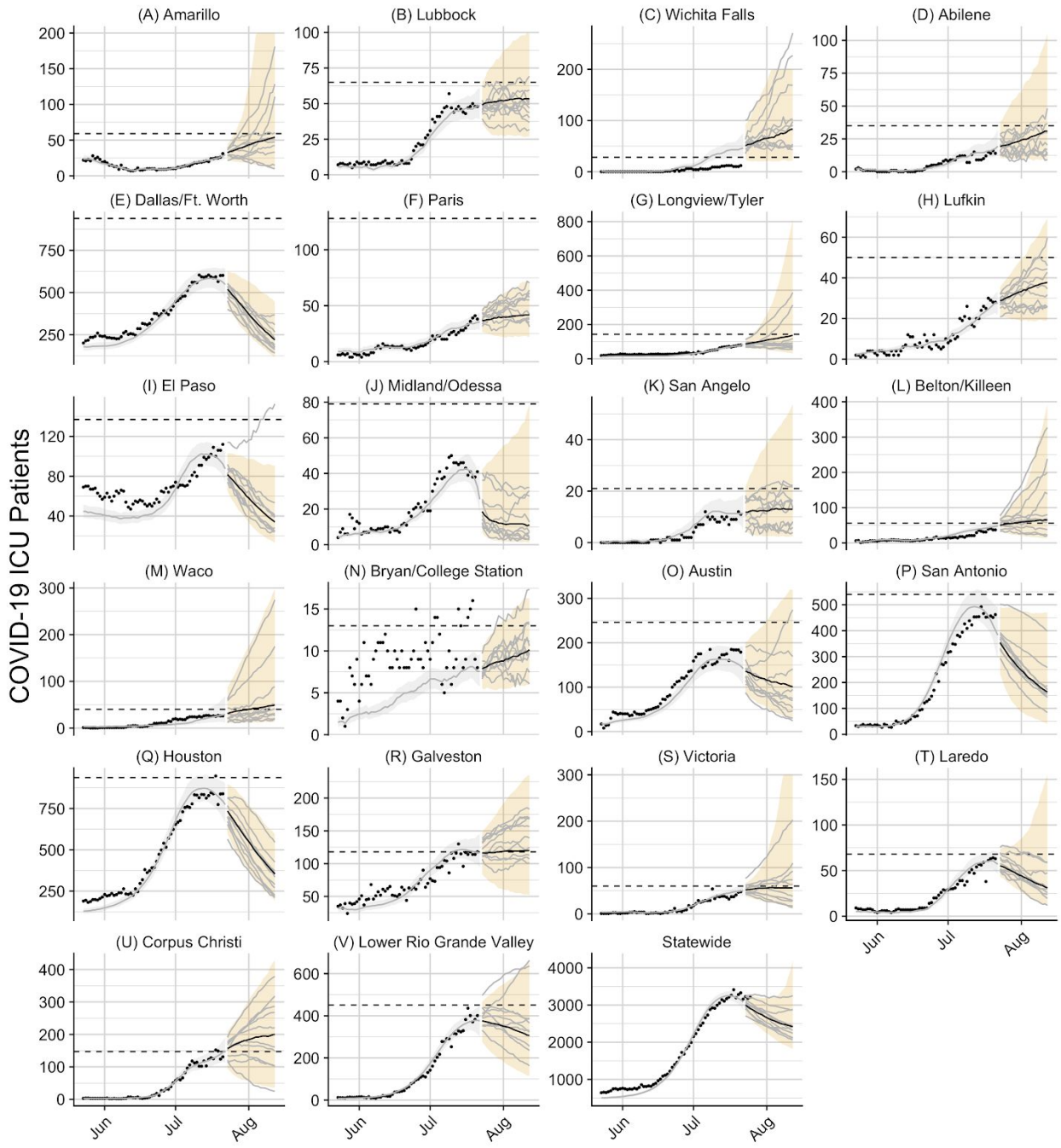

Figure 3: Projected COVID-19 ICU patients through August 12, 2020 by TSA. Black points represent the reported daily COVID-19 ICU census provided by DSHS. Grey "spaghetti" lines represent equally likely projections and the black line indicates the median trend based on the range of transmission rates estimated for July 22-August 12, 2020 (Table 1). Differences between lines are caused by uncertainty in the model inputs as well as variation in individual behavior and disease progression. These projections assume a TSA-specific ratio of ICU bed usage to hospital bed usage based on ratios calculated on July 21, 2020. Horizontal dashed lines indicate the estimated TSA-specific ICU bed capacity (obtained by summing used and available ICU beds).

Appendix

COVID-19 Epidemic Model Structure and Parameters

The model structure is diagrammed in Figure A1 and described in the equations below.
For each age and risk group, we build a separate set of compartments to model the transitions between the states: susceptible (S), exposed (E), pre-symptomatic infectious (P^Y), pre-asymptomatic infectious (P^A), symptomatic infectious (I^Y), asymptomatic infectious (I^A), symptomatic infectious that are hospitalized (I^H), and recovered (R). The symbols S, E, P^Y, P^A, I^Y, I^A, I^H, and R denote the number of people in that state in the given age/risk group and the total size of the age/risk group is

$$.N = S + E + P^Y + P^A + I^Y + I^A + I^H + R$$

The deterministic model for individuals in age group a and risk group r is given by:

$$\frac{dS_{a,r}}{dt} = -S_{a,r} \cdot \sum_{i \in A} \sum_{j \in K} (I^Y_{i,j}\omega^Y + I^A_{i,j}\omega^A + P^Y_{i,j}\omega^{PY} + P^A_{i,j}\omega^{PA})\beta(t)\phi_{a,i}/N_i$$

$$\frac{dE_{a,r}}{dt} = S_{a,r} \cdot \sum_{i \in A} \sum_{j \in K} (I^Y_{i,j}\omega^Y + I^A_{i,j}\omega^A + P^Y_{i,j}\omega^{PY} + P^A_{i,j}\omega^{PA})\beta(t)\phi_{a,i}/N_i - \sigma E_{a,r}$$

$$\frac{dP^A_{a,r}}{dt} = (1-\tau)\sigma E_{a,r} - \rho^A P^A_{a,r}$$

$$\frac{dP^Y_{a,r}}{dt} = \tau\sigma E_{a,r} - \rho^Y P^Y_{a,r}$$

$$\frac{dI^A_{a,r}}{dt} = \rho^A P^A_{a,r} - \gamma^A I^A_{a,r}$$

$$\frac{dI^Y_{a,r}}{dt} = \rho^Y P^Y_{a,r} - (1-\pi)\gamma^Y I^Y_{a,r} - \pi\eta I^Y_{a,r}$$

$$\frac{dI^H_{a,r}}{dt} = \pi\eta I^Y_{a,r} - \gamma^H(t) I^H_{a,r}$$

$$\frac{dR_{a,r}}{dt} = \gamma^A I^A_{a,r} + (1-\pi)\gamma^Y I^Y_{a,r} + \gamma^H(t) I^H_{a,r}$$

where A and K are all possible age and risk groups, ^{A}, ^{Y}, ^{PA}, ω^{PY} are the relative infectiousness of the I^A, I^Y, I^{PA}, I^{PY} compartments, respectively, β is transmission rate, $_{a,i}$ is the mixing rate between age group a, $i \in A$, and γ^A, γ^Y, $\gamma^H(t)$ are the recovery rates for the I^A, I^Y, I^H compartments, respectively, σ is the exposed rate, ρ^A, ρ^Y are the pre-(a)symptomatic rates, τ is the symptomatic ratio, and π is the proportion of symptomatic individuals requiring hospitalization.

We simulate the model using a stochastic implementation of the deterministic equations. Transitions between compartments are governed using the τ-leap method [3,4] with key parameters given in Table A1-2. We simulate the model according to the following equations:

$$S_{a,r}(t+1) - S_{a,r}(t) = -P_1$$
$$E_{a,r}(t+1) - E_{a,r}(t) = P_1 - P_2$$
$$P^A_{a,r}(t+1) - P^A_{a,r}(t) = (1-\tau)P_2 - P_3$$
$$P^Y_{a,r}(t+1) - P^Y_{a,r}(t) = \tau P_2 - P_4$$
$$I^A_{a,r}(t+1) - I^A_{a,r}(t) = P_3 - P_5$$
$$I^Y_{a,r}(t+1) - I^Y_{a,r}(t) = P_4 - P_6 - P_7$$
$$I^H_{a,r}(t+1) - I^H_{a,r}(t) = P_7 - P_8$$
$$R_{a,r}(t+1) - R_{a,r}(t) = P_5 + P_6 + P_8$$

with

$$P_1 \sim B(n = S_{a,r}(t),\, p = 1 - e^{-(F_{a,r}(t))\cdot dt})$$
$$P_2 \sim B(n = E_{a,r}(t),\, p = 1 - e^{-(\sigma)\cdot dt})$$
$$P_3 \sim B(n = P^A_{a,r}(t),\, p = 1 - e^{-(\rho^A)\cdot dt})$$
$$P_4 \sim B(n = P^Y_{a,r}(t),\, p = 1 - e^{-(\rho^Y)\cdot dt})$$
$$P_5 \sim B(n = I^A_{a,r}(t),\, p = 1 - e^{-(\gamma^A)\cdot dt})$$
$$P_6 \sim B(n = I^Y_{a,r}(t),\, p = 1 - e^{-((1-\pi)\gamma^Y)\cdot dt})$$
$$P_7 \sim B(n = I^Y_{a,r}(t),\, p = 1 - e^{-(\pi\eta)\cdot dt})$$
$$P_8 \sim B(n = I^H_a,\, p = 1 - e^{-\gamma^H(t)\cdot dt})$$

where *B*(*n*,*p*) denotes a binomial distribution with *n* trials each with probability of success *p*. $F_{a,r}$ denotes the force of infection for individuals in age group a and risk group r and is given by

$$F_{a,r}(t) = \sum_{i\in A}\sum_{j\in K}(I^Y_{i,r}(t)\omega^Y + I^A_{i,r}(t)\omega^A + P^Y_{i,j}(t)\omega^{PY} + P^A_{i,j}(t)\omega^{PA})\beta(t)\phi_{a,i}/N_i$$

with

$$\beta(t) = \beta(0)e^{b_1(t)\cdot PC1 + Z(t)}$$
$$b_1(t) \sim N(b_1(t-1), \sigma_{b_1})$$
$$Z(t) \sim N(0.97\cdot Z(t-1), \sigma_Z),\ Z(0) = 0.$$

where PC1 describes the first principal components from our mobility data as described below. Finally,

$\gamma^H(t) = \text{expit}(\log(\gamma^H(0)) + Z_\gamma)$ where $Z_\gamma(t) \sim N(Z_\gamma(t-1), \sigma_\gamma),\ Z\gamma(0) = 0.$

We estimate $\beta(t)$, k, σ_Z, $b_1(t)$, σ_{b_1}, ψ_μ, σ_μ, and σ_γ as described in the model fitting section below.

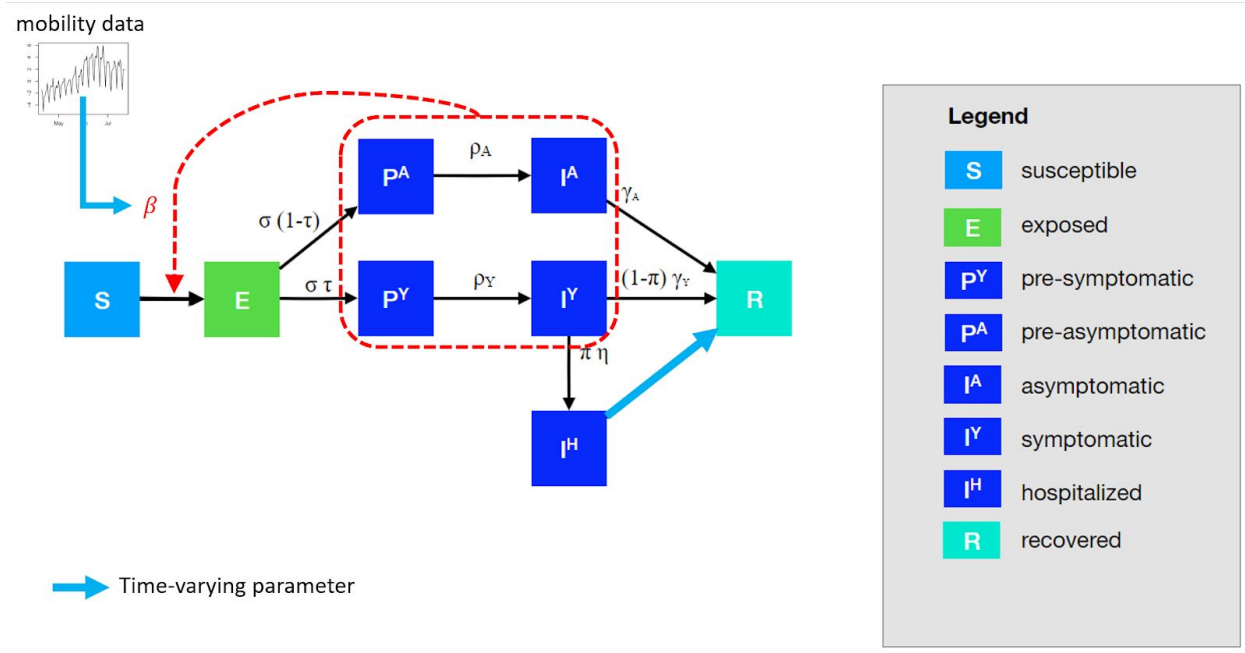

Figure A1. Compartmental model of COVID-19 transmission. Each subgroup (defined by age and risk) is modeled with a separate set of compartments. Upon infection, susceptible individuals (*S*) progress to exposed (*E*) and then to either pre-symptomatic infectious (P^Y) or pre-asymptomatic infectious (P^A) from which they move to symptomatic infectious (I^Y) and asymptomatic infectious (I^A) respectively. All asymptomatic cases eventually progress to a recovered class where they remain protected from future infection (*R*); symptomatic cases are either hospitalized (I^H) or recover.

Mobility trends

We used mobility trends data for each TSA to inform the transmission rate in our model. Specifically, we ran a principal component analysis (PCA) on eight independent mobility variables provided by SafeGraph, including home dwell time and visits to universities, bars, grocery stores, museums and parks, medical facilities, schools, and restaurants [2]. We regressed the transmission rate on the first two principal components from the mobility data as described in the modeling equations for $\beta(t)$.

Epidemic starting conditions

The epidemic starting condition are governed by two fitted parameters, E_0, and H_0, and initial ratios of all compartments taken from early epidemic ratios of the Austin model. E_0 scales the compartments outside the hospital, and H_0 in the hospital. Each compartment is initialized by using the Poisson distribution. Thus the initial state of the E compartment will be

$$E_{a,r}(0) \sim \text{Poisson}(E_0 r_{E,a,r})$$

And the H compartment will be

$$H_{a,r}(0) \sim \text{Poisson}(H_0 r_{H,a,r})$$

Model likelihood

We obtained daily hospital admit ($H_A(t)$), and total hospitalizations ($H(t)$) for each of the Texas TSAs. In this model we estimated E_0, H_0, β_0, $b_1(t)$, σ_{b_1}, r, r_A, $\gamma_H(t)$, γ_{H0}, σ_γ, $Z(t)$, σ_Z and fixed the remaining parameters as described in Table A1-2. We assumed all sources of data were negative binomially distributed around their predicted values from the SEIR stochastic model, and chose informative, but relatively dispersed priors for certain parameters for stability in parameter estimation and to prevent the model from overfitting data through large perturbations to time-dependent variables.

Following all of these considerations, the likelihood for our stochastic model was:

$$p(Y(t), b_1(0), \sigma_{b_1}, b_2(0), \sigma_{b_2}, k|\theta) = p(Y(t)|\theta, b_1(0), \sigma_{b_1}, b_2(0), \sigma_{b_2}, k) \cdot p(\theta, b_1(0), \sigma_{b_1}, b_2(0), \sigma_{b_2}, k)$$

where $Y(t)$ refers to the two types of data from hospitals, θ contains all parameters from Table A1 not explicitly listed, and where

$$p(Y(t)|\theta, b_1(0), \sigma_{b_1}, b_2(0), \sigma_{b_2}, k) = p(H_A(t)|\hat{H}_A(t)) p(H(t)|\hat{H}(t))$$
$$p(\theta, b_1(0), \sigma_{b_1}, b_2(0), \sigma_{b_2}, k) = p(b_1(0)) \cdot p(\sigma_{b_1}) \cdot p(b_2(0)) \cdot p(\sigma_{b_2}) \cdot p(k)$$

with

$$p(H_A(t)|\hat{H}_A(t)) = \frac{\Gamma(r_A + H_A(t))}{H_A(t)! \cdot \Gamma(r)} \left(\frac{r_A}{r_A + \hat{H}_A(t)}\right)^{r_A} \left(\frac{\hat{H}_A(t)}{r_A + \hat{H}_A(t)}\right)^{H_A(t)}$$

$$p(H(t)|\hat{H}(t)) = \frac{\Gamma(r + H(t))}{H(t)! \cdot \Gamma(r)} \left(\frac{r}{r + \hat{H}(t)}\right)^{r} \left(\frac{\hat{H}(t)}{r + \hat{H}(t)}\right)^{H(t)}$$

I.e. negative binomials with means $\hat{H}(t)$ and $\hat{H}_A(t)$, and dispersion parameters r and r_A.

$$p(b_1(0)) \cdot t_d = \frac{1}{\sqrt{2}} e^{-\frac{1}{2}(\hat{b}_1(0))^2}$$

$$p(\gamma_H(0)) \cdot t_d = \frac{1}{\sqrt{2}} e^{-\frac{1}{2}(\hat{\gamma}_H(0))^2}$$

$$p(\sigma_{b_1}) \cdot t_d = \frac{1}{\Gamma(1.1) \cdot \frac{1}{1.1}^{1.1}} \sigma_{b_1}^{1.1-1} e^{-1.1 \cdot \sigma_{b_1}}$$

$$p(\sigma_{\gamma_H}) \cdot t_d = \frac{1}{\Gamma(1.1) \cdot \frac{1}{1.1}^{1.1}} \sigma_{\gamma_H}^{1.1-1} e^{-1.1 \cdot \sigma_{\gamma_H}}$$

$$p(r) \cdot t_d = e^r$$

$$p(r_A) \cdot t_d = e^{r_A}$$

and t_d is the number of days in the fitting time period.

Fitting method

In this model we estimated E_0, H_0, β_0, $b_1(t)$, σ_{b_1}, r, r_A, $\gamma_H(t)$, γ_{H0}, σ_γ, $Z(t)$, σ_Z and fixed the remaining parameters as described in Table A1. Fitting was carried out using the iterated filtering algorithm made available through the mif2 function in the pomp package in R [6,7]. This algorithm is a stochastic optimization procedure; it performs maximum likelihood estimation using a particle filter to provide a noisy estimate of the likelihood for a given combination of the parameters. For each parameter combination we ran 50 bouts of 300 iterations of iterated filtering, each with 3,500 particles and chose the best of 50 in terms of likelihood. We calculated smoothed posterior estimates for all of the states within the model through time (including $\beta(t)$ and other time-dependent parameters which are technically state variables in our model formulation, as it changes through time according to a stochastic process). We calculated these smoothed posteriors as follows:

1. We ran 10,000 independent particle filters at the MLE, each with 2,500 particles. For each run, l, of particle filtering, we kept track of the complete trajectory of each particle, as well as the filtered estimate of the likelihood, L_l.
2. For each of the 10,000 particle filtering runs, we randomly sampled a single complete particle trajectory, giving us 10,000 separate trajectories for all state variables.
3. We resampled from these 10,000 trajectories 500 trajectories with probabilities proportional to L_l to give a distribution of state trajectories

The result can be thought of as an empirical-Bayes posterior distribution: that is, a set of 500 smoothed posterior draws from all state variables, conditional on the maximum likelihood estimates for the model's free parameters. This smoothed posterior distribution is how we calculate means and credible intervals for $\beta(t)$ in addition to all other time-varying state variables.

To estimate future trajectories, we took each of the sampled 500 smoothed posterior draws, and continued the trajectory into the future starting from the states at the end of the trajectory. The time-varying parameters were fixed in each of these trajectories to their fitted value at the most recent date of data.

Table A1. Model parameters[a]

Parameters	Value	Source
Start date	April 11, 2020	Start of data
Initial infections	fitted	
$\beta(t)$: daily transmission rate	N/A	Estimated
γ^A: recovery rate on asymptomatic compartment	Equal to γ^Y	Assumption
γ^Y: recovery rate on symptomatic non-treated compartment	0.25	He et al. [8]
τ: symptomatic proportion (%)	57	Fox et al. [9]
σ: exposed rate	1/2.9	Zhang et al. [10]; He et al. [8]
ρ^A: pre-asymptomatic rate	Equal to ρ^Y	
ρ^Y: pre-symptomatic rate	$\frac{1}{2.3}$	He et al. [8]
P: proportion of pre-symptomatic transmission	44%	He et al. [8]
ω^P: relative infectiousness of pre-symptomatic individuals	$\omega^P = \frac{P}{1-P}\frac{\tau\omega^Y[YHR/\eta+(1-YHR)/\gamma^Y]+(1-\tau)\omega^A/\gamma^A}{\tau\omega^Y/\rho^Y+(1-\tau)\omega^A/\rho^A}$ $\omega^{PY} = \omega^P\omega^Y, \omega^{PA} = \omega^P\omega^A$	
ω^A: relative infectiousness of infectious individuals in compartment I^A	$\frac{2}{3}$	He et al. [11]
h: high-risk proportion, age specific (%)	[8.2825, 14.1121, 16.5298, 32.9912, 47.0568]	Estimated using 2015-2016 Behavioral Risk Factor Surveillance System (BRFSS) data with multilevel regression and poststratification using CDC's list of conditions that may increase the risk of serious complications from influenza [13–15]

[a]Values given as five-element vectors are age-stratified with values corresponding to 0-4, 5-17, 18-49, 50-64, 65+ year age groups, respectively.

Table A2 Hospitalization parameters

Parameters	Value	Source
$\gamma^H(t)$: recovery rate in hospitalized compartment	Fitted	
YHR: symptomatic case hospitalization rate (%)	Low risk: [0.04021, 0.03091, 1.903, 4.114, 4.879] High risk: [0.4021, 0.3091, 19.03, 41.14, 48.79]	Age adjusted from Verity et al. [12]
π: rate of symptomatic individuals go to hospital, age-specific	$\pi = \frac{\gamma^Y * YHR}{\eta + (\gamma^Y - \eta)YHR}$	
η: rate from symptom onset to hospitalized	0.1695	5.9 day average from symptom onset to hospital admission Tindale et al. [16]
ICU: proportion hospitalized people in ICU	Varies for each TSA based on calculated percent on July 21, 2020	Estimated from DSHS COVID-19 hospitalization data

Table A3 Contact matrix. Daily number contacts by age group on an average day.

	0-4y	5-17y	18-49y	50-64y	65y+
0-4y	1.88	2.02	4.01	0.79	0.28
5-17y	0.55	7.06	5.02	0.70	0.22
18-49y	0.37	2.19	8.72	1.45	0.21
50-64y	0.33	1.62	5.79	2.79	0.50
65y+	0.19	0.88	2.36	1.19	1.22

Estimation of age-stratified proportion of population at high-risk for COVID-10 complications

We estimate age-specific proportions of the population at high risk of complications from COVID-19 based on data for cities of the largest MSA in each of the TSA, from the the CDC's 500 cities project (Figure A2) [17], or on the Texas average when no MSA is in the TSA. We assume that high risk conditions for COVID-19 are the same as those specified for influenza by the CDC [13]. The CDC's 500 cities project provides city-specific estimates of prevalence for several of these conditions among adults [18]. The estimates were obtained from the 2015-2016

Behavioral Risk Factor Surveillance System (BRFSS) data using a small-area estimation methodology called multi-level regression and poststratification [14,15]. It links geocoded health surveys to high spatial resolution population demographic and socioeconomic data [15].

Estimating high-risk proportions for adults. To estimate the proportion of adults at high risk for complications, we use the CDC's 500 cities data, as well as data on the prevalence of HIV/AIDS, obesity and pregnancy among adults (Table A6).

The CDC 500 cities dataset includes the prevalence of each condition on its own, rather than the prevalence of multiple conditions (e.g., dyads or triads). Thus, we use separate co-morbidity estimates to determine overlap. Reference about chronic conditions [19] gives US estimates for the proportion of the adult population with 0, 1 or 2+ chronic conditions, per age group. Using this and the 500 cities data we can estimate the proportion of the population p_{HR} in each age group in each city with at least one chronic condition listed in the CDC 500 cities data (Table A6) putting them at high-risk for flu complications.

HIV: We use the data from table 20a in CDC HIV surveillance report [20] to estimate the population in each risk group living with HIV in the US (last column, 2015 data). Assuming independence between HIV and other chronic conditions, we increase the proportion of the population at high-risk for influenza to account for individuals with HIV but no other underlying conditions.

Morbid obesity: A BMI over 40kg/m^2 indicates morbid obesity, and is considered high risk for influenza. The 500 Cities Project reports the prevalence of obese people in each city with BMI over 30kg/m^2 (not necessarily morbid obesity). We use the data from table 1 in Sturm and Hattori [21] to estimate the proportion of people with BMI>30 that actually have BMI>40 (across the US); we then apply this to the 500 Cities obesity data to estimate the proportion of people who are morbidly obese in each city. Table 1 of Morgan et al. [22] suggests that 51.2% of morbidly obese adults have at least one other high risk chronic condition, and update our high-risk population estimates accordingly to account for overlap.

Pregnancy: We separately estimate the number of pregnant women in each age group and each city, following the methodology in CDC reproductive health report [23]. We assume independence between any of the high-risk factors and pregnancy, and further assume that half the population are women.

Estimating high-risk proportions for children. Since the 500 Cities Project only reports data for adults 18 years and older, we take a different approach to estimating the proportion of children at high risk for severe influenza. The two most prevalent risk factors for children are asthma and obesity; we also account for childhood diabetes, HIV and cancer.
From Miller et al. [24], we obtain national estimates of chronic conditions in children. For asthma, we assume that variation among cities will be similar for children and adults. Thus, we use the relative prevalences of asthma in adults to scale our estimates for children in each city.

The prevalence of HIV and cancer in children are taken from CDC HIV surveillance report [20] and cancer research report [25], respectively.

We first estimate the proportion of children having either asthma, diabetes, cancer or HIV (assuming no overlap in these conditions). We estimate city-level morbid obesity in children using the estimated morbid obesity in adults multiplied by a national constant ratio for each age group estimated from Hales et al. [26], this ratio represents the prevalence in morbid obesity in children given the one observed in adults. From Morgan et al. [22], we estimate that 25% of morbidly obese children have another high-risk condition and adjust our final estimates accordingly.

Resulting estimates. We compare our estimates for the Austin-Round Rock Metropolitan Area to published national-level estimates [27] of the proportion of each age group with underlying high risk conditions (Table A6). The biggest difference is observed in older adults, with Austin having a lower proportion at risk for complications for COVID-19 than the national average; for 25-39 year olds the high risk proportion is slightly higher than the national average.

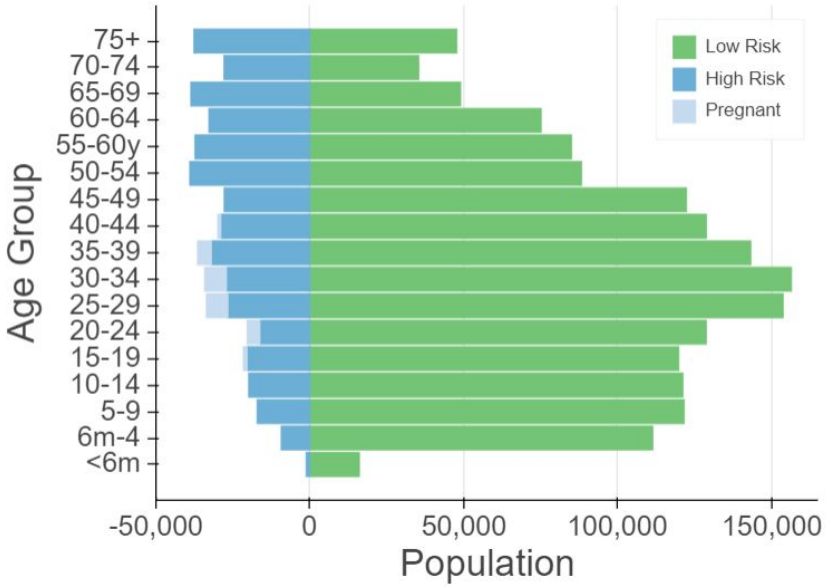

Figure A2. Demographic and risk composition of the Austin-Round Rock MSA. Bars indicate age-specific population sizes, separated by low risk, high risk, and pregnant. High risk is defined as individuals with cancer, chronic kidney disease, COPD, heart disease, stroke, asthma, diabetes, HIV/AIDS, and morbid obesity, as estimated from the CDC 500 Cities Project [17], reported HIV prevalence [20] and reported morbid obesity prevalence [21,22], corrected for multiple conditions. The population of pregnant women is derived using the CDC's method combining fertility, abortion and fetal loss rates [28–30].

Table A4. High-risk conditions for influenza and data sources for prevalence estimation

Condition	Data source
Cancer (except skin), chronic kidney disease, COPD, coronary heart disease, stroke, asthma, diabetes	CDC 500 cities [17]
HIV/AIDS	CDC HIV Surveillance report [20]
Obesity	CDC 500 cities [17], Sturm and Hattori [21], Morgan et al. [22]
Pregnancy	National Vital Statistics Reports [28] and abortion data [29]

Table A5. Comparison between published national estimates and Austin-Round Rock MSA estimates of the percent of the population at high-risk of influenza/COVID-19 complications.

Age Group	National estimates [26]	Austin-Round Rock (excluding pregnancy)	Pregnant women (proportion of age group)
0 to 6 months	NA	8.1	-
6 months to 4 years	6.8	9.0	-
5 to 9 years	11.7	14.6	-
10 to 14 years	11.7	16.7	-
15 to 19 years	11.8	17.0	3.2
20 to 24 years	12.4	13.2	10.6
25 to 34 years	15.7	17.4	9.6
35 to 39 years	15.7	22.1	3.7
40 to 44 years	15.7	22.5	0.6
45 to 49 years	15.7	22.7	-
50 to 54 years	30.6	37.5	-
55 to 60 years	30.6	37.4	-
60 to 64 years	30.6	37.3	-
65 to 69 years	47.0	53.2	-
70 to 74 years	47.0	53.2	-
75 years and older	47.0	53.2	-

Trauma Service Areas in Texas

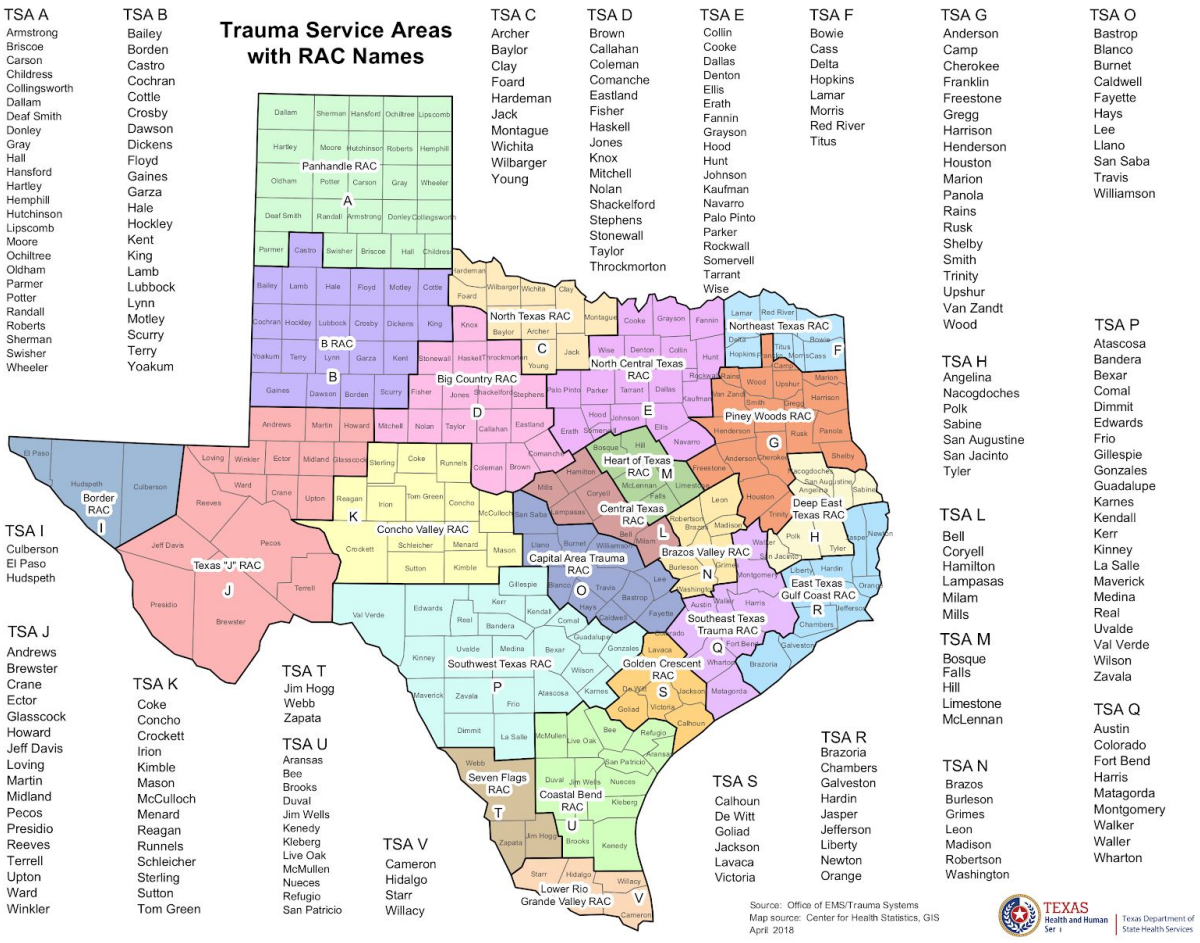

Figure AN. Map of Trauma Service Areas with RAC Names obtained from DSHS: https://www.dshs.texas.gov/emstraumasystems/etrarac.shtm.

References

1. Seventh Amended Emergency Order for Public Health Emergency due to COVID-19. [cited 28 Apr 2020]. Available: https://co.jefferson.tx.us/documents/Coronavirus%20Docs/coronavirusdocs.htm

1. Ionides EL, Nguyen D, Atchadé Y, Stoev S, King AA. Inference for dynamic and latent variable models via iterated, perturbed Bayes maps. Proc Natl Acad Sci U S A. 2015;112: 719–724.

2. Gao S, Rao J, Kang Y, Liang Y, Kruse J. Mapping county-level mobility pattern changes in the United States in response to COVID-19. arXiv [physics.soc-ph]. 2020. Available:

http://arxiv.org/abs/2004.04544

3. Keeling MJ, Rohani P. Modeling Infectious Diseases in Humans and Animals. Princeton University Press; 2011.

4. Gillespie DT. Approximate accelerated stochastic simulation of chemically reacting systems. J Chem Phys. 2001;115: 1716–1733.

5. Liu Y, Gayle AA, Wilder-Smith A, Rocklöv J. The reproductive number of COVID-19 is higher compared to SARS coronavirus. J Travel Med. 2020;27. doi:10.1093/jtm/taaa021

6. R Core Team. R: A Language and Environment for Statistical Computing. Vienna, Austria: R Foundation for Statistical Computing; 2020. Available: https://www.R-project.org/

7. King AA, Nguyen D, Ionides EL. Statistical Inference for Partially Observed Markov Processes via the R Package pomp. arXiv [stat.ME]. 2015. Available: http://arxiv.org/abs/1509.00503

8. He X, Lau EHY, Wu P, Deng X, Wang J, Hao X, et al. Temporal dynamics in viral shedding and transmissibility of COVID-19. Nat Med. 2020. doi:10.1038/s41591-020-0869-5

9. Fox SJ, Pasco R, Tec M, Du Z, Lachmann M, Scott J, et al. The impact of asymptomatic COVID-19 infections on future pandemic waves. medRxiv. 2020. Available: https://www.medrxiv.org/content/10.1101/2020.06.22.20137489v1.abstract

10. Zhang J, Litvinova M, Wang W, Wang Y, Deng X, Chen X, et al. Evolving epidemiology and transmission dynamics of coronavirus disease 2019 outside Hubei province, China: a descriptive and modelling study. Lancet Infect Dis. 2020. doi:10.1016/S1473-3099(20)30230-9

11. He D, Zhao S, Lin Q, Zhuang Z, Cao P, Wang MH, et al. The relative transmissibility of asymptomatic COVID-19 infections among close contacts. Int J Infect Dis. 2020;94: 145–147.

12. Verity R, Okell LC, Dorigatti I, Winskill P, Whittaker C, Imai N, et al. Estimates of the severity of COVID-19 disease. Epidemiology. medRxiv; 2020. doi:10.1101/2020.03.09.20033357

13. CDC. People at High Risk of Flu. In: Centers for Disease Control and Prevention [Internet]. 1 Nov 2019 [cited 26 Mar 2020]. Available: https://www.cdc.gov/flu/highrisk/index.htm

14. CDC - BRFSS. 5 Nov 2019 [cited 26 Mar 2020]. Available: https://www.cdc.gov/brfss/index.html

15. Zhang X, Holt JB, Lu H, Wheaton AG, Ford ES, Greenlund KJ, et al. Multilevel regression and poststratification for small-area estimation of population health outcomes: a case study of chronic obstructive pulmonary disease prevalence using the behavioral risk factor surveillance system. Am J Epidemiol. 2014;179: 1025–1033.

16. Tindale L, Coombe M, Stockdale JE, Garlock E, Lau WYV, Saraswat M, et al. Transmission interval estimates suggest pre-symptomatic spread of COVID-19. Epidemiology. medRxiv;

2020. doi:10.1101/2020.03.03.20029983

17. 500 Cities Project: Local data for better health | Home page | CDC. 5 Dec 2019 [cited 19 Mar 2020]. Available: https://www.cdc.gov/500cities/index.htm

18. Health Outcomes | 500 Cities. 25 Apr 2019 [cited 28 Mar 2020]. Available: https://www.cdc.gov/500cities/definitions/health-outcomes.htm

19. Part One: Who Lives with Chronic Conditions. In: Pew Research Center: Internet, Science & Tech [Internet]. 26 Nov 2013 [cited 23 Nov 2019]. Available: https://www.pewresearch.org/internet/2013/11/26/part-one-who-lives-with-chronic-conditions/

20. for Disease Control C, Prevention, Others. HIV surveillance report. 2016; 28. URL: http://www cdc gov/hiv/library/reports/hiv-surveil-lance html Published November. 2017.

21. Sturm R, Hattori A. Morbid obesity rates continue to rise rapidly in the United States. Int J Obes . 2013;37: 889–891.

22. Morgan OW, Bramley A, Fowlkes A, Freedman DS, Taylor TH, Gargiullo P, et al. Morbid obesity as a risk factor for hospitalization and death due to 2009 pandemic influenza A(H1N1) disease. PLoS One. 2010;5: e9694.

23. Estimating the Number of Pregnant Women in a Geographic Area from CDC Division of Reproductive Health. Available: https://www.cdc.gov/reproductivehealth/emergency/pdfs/PregnacyEstimatoBrochure508.pdf

24. Miller GF, Coffield E, Leroy Z, Wallin R. Prevalence and Costs of Five Chronic Conditions in Children. J Sch Nurs. 2016;32: 357–364.

25. Cancer Facts & Figures 2014. [cited 30 Mar 2020]. Available: https://www.cancer.org/research/cancer-facts-statistics/all-cancer-facts-figures/cancer-facts-figures-2014.html

26. Hales CM, Fryar CD, Carroll MD, Freedman DS, Ogden CL. Trends in Obesity and Severe Obesity Prevalence in US Youth and Adults by Sex and Age, 2007-2008 to 2015-2016. JAMA. 2018;319: 1723–1725.

27. Zimmerman RK, Lauderdale DS, Tan SM, Wagener DK. Prevalence of high-risk indications for influenza vaccine varies by age, race, and income. Vaccine. 2010;28: 6470–6477.

28. Martin JA, Hamilton BE, Osterman MJK, Driscoll AK, Drake P. Births: Final Data for 2017. Natl Vital Stat Rep. 2018;67: 1–50.

29. Jatlaoui TC, Boutot ME, Mandel MG, Whiteman MK, Ti A, Petersen E, et al. Abortion Surveillance - United States, 2015. MMWR Surveill Summ. 2018;67: 1–45.

30. Ventura SJ, Curtin SC, Abma JC, Henshaw SK. Estimated pregnancy rates and rates of pregnancy outcomes for the United States, 1990-2008. Natl Vital Stat Rep. 2012;60: 1–21.